

# Electronically monitoring biological interactions with carbon nanotube field-effect transistors

Douglas R. Kauffman<sup>ab</sup> and Alexander Star<sup>\*ab</sup>

Received 18th February 2008

First published as an Advance Article on the web 7th April 2008

DOI: 10.1039/b709567h

The year 2008 marks the 10th anniversary of the carbon nanotube field-effect transistor (NTFET). In the past decade a vast amount of effort has been placed on the development of NTFET based sensors for the detection of both chemical and biological species. Towards this end, NTFETs show great promise because of their extreme environmental sensitivity, small size, and ultra-low power requirements. Despite the great progress NTFETs have shown in the field of biological sensing, debate still exists over the mechanistic origins underlying the electronic response of NTFET devices, specifically whether analyte species interact with the carbon nanotube conduction channel or if interaction with the NTFET electrodes actually triggers device response. In this *tutorial review*, we describe the fabrication of NTFET devices, and detail several reports that illustrate recent advances in biological detection using NTFET devices, while highlighting the suggested mechanisms explaining the device response to analyte species. In doing this we hope to show that NTFET technology has the potential for low-cost and portable bioanalytical platforms.

## Introduction

Nanotube field-effect transistors (NTFETs) were independently reported in 1998 by both the Dekker group<sup>1</sup> at Delft University and the Avouris group<sup>2</sup> at IBM. NTFET devices are unique in the world of semiconductor-based transistors because their conduction channel consists of carbon nanotubes (CNTs). The incorporation of CNTs into electronic circuitry has allowed NTFET devices to be developed into sensor platforms with unrivaled sensitivity towards local chemical environments. CNTs composed of a single cylindrical layer of carbon atoms, called single-walled carbon nano-

tubes (SWNTs), have found promising use in sensor applications because their electrical conductivity can be modified through interaction with chemical<sup>3</sup> or biological<sup>4</sup> species. Furthermore, the small diameter and relatively long length ( $\mu\text{m}$ ) of SWNTs allows them to probe molecular systems on a local scale by directly “wiring into” individual or small assemblies of molecules. These characteristics of SWNT based NTFETs create unique platforms for studying molecular systems with unsurpassed sensitivity.

## Integrating SWNTs into electronic devices

Depending on the arrangement of carbon atoms along the tube length, a SWNT will either be metallic or semiconducting.<sup>5</sup> Under ambient conditions, semiconducting SWNTs

<sup>a</sup> Department of Chemistry, University of Pittsburgh, Pittsburgh, PA 15260, USA. E-mail: astar@pitt.edu

<sup>b</sup> National Energy Technology Lab, Pittsburgh, PA 15236, USA



Douglas R. Kauffman

Douglas R. Kauffman graduated with a BS in Chemistry from the University of Pittsburgh in 2005. He remained there to pursue a PhD in the Department of Chemistry under the guidance of Prof. Alexander Star where he studies the design and operation of nanomaterial-based electronic devices and chemical sensors. Currently he is investigating the optical spectroscopy and solid-state electronic properties of single-walled carbon nanotube networks under chemical interactions.



Alexander Star

Alexander Star received a PhD in supramolecular chemistry from Tel Aviv University in 2000. He spent two years as a postdoctoral associate in Prof. J. Fraser Stoddart's California Nano-Systems Institute group at the University of California, Los Angeles. He was employed as a Senior Scientist at Nanomix, Inc. for three years developing carbon nanotube-based sensors. As an assistant Professor of Chemistry at the University of Pittsburgh since 2005 his research interests include molecular recognition at the nanoscale, and nanotechnology enabled molecular sensing.

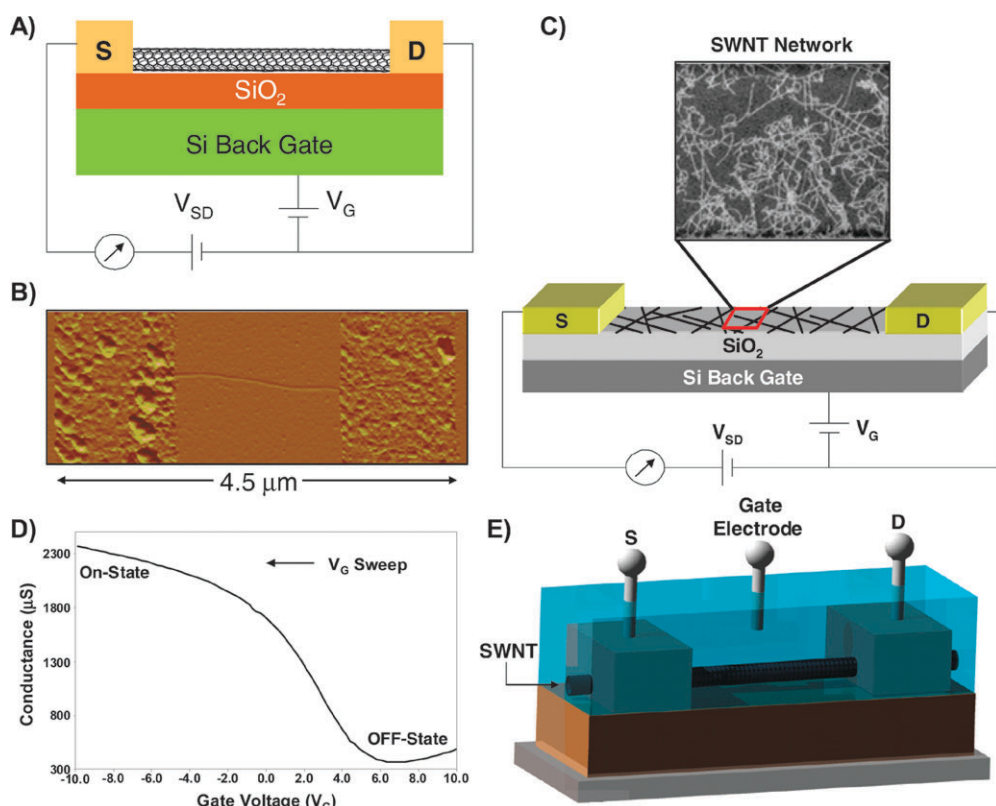


**Fig. 1** (A) A NTFET device composed of an isolated SWNT between source (S) and drain (D) electrodes on top of a SiO<sub>2</sub> substrate with an underlying Si gate electrode. (B) Atomic force microscope (AFM) image of the NTFET device illustrated in part A. (C) NTFET device composed of a random network of SWNTs as the conduction channel, with a scanning electron microscope (SEM) image of the SWNT network; the SEM image width is 10 μm. (D) NTFET transistor characteristic showing the source–drain conductance *versus* gate voltage ( $G-V_G$ ) curve obtained by sweeping the gate voltage from +10 to –10 V at a constant S–D bias voltage ( $V_{SD}$ ) of 0.05 V using a NTFET with a random network of SWNTs between interdigitated Ti/Au electrodes on a SiO<sub>2</sub> insulated Si back gate. (E) A liquid gated NTFET where the electrochemical potential of the solution is controlled with a gate electrode. (Parts A and B are reproduced with permission from ref. 4, copyright 2007 Wiley-VCH Verlag GmbH & Co. KGaA.)

demonstrate p-type electrical behavior, which enables them to conduct holes instead of electrons; this is widely believed to result from oxygen adsorption on the SWNT<sup>6</sup> or at the device electrode.<sup>7</sup> To function in an electronic device, the SWNT must be contacted to a metal electrode. If the semiconducting SWNT and metal have different work functions, then Fermi level equilibration will occur;<sup>8</sup> this phenomenon leads to a donation of electronic density from the metal into the partially depleted SWNT valence band. At the SWNT–metal interface a region of increased electronic density forms in the SWNT valence band called a depletion region, and a potential barrier, called a Schottky barrier (SB), inhibits the transmission of holes from the metal electrode into the SWNT.

In a NTFET, the SWNT (or network of SWNTs<sup>9</sup>) acts as a conduction channel between two electrodes. Current flow through the SWNT conduction channel is modulated by an external electric field applied through a so called “gate electrode”. Fig. 1A represents a NTFET composed of an isolated SWNT as the conduction channel. Here the SWNT lies on top of a conductive Si substrate covered with a thin insulating SiO<sub>2</sub> layer. Two metal electrodes act as the source (S) and drain (D) electrodes that are held at a constant bias voltage ( $V_{SD}$ ), and the bottom Si substrate acts as the insulated back gate electrode. Fig. 1B is an atomic force microscope (AFM) image of such a NTFET device where an isolated SWNT bridges the

S–D electrodes on top of a SiO<sub>2</sub> substrate with a Si back gate (not visible). Current modulation is achieved by sweeping the gate voltage between positive and negative values. Towards very positive gate voltages, the SB at the SWNT–metal electrode inhibits the transport of holes from the metal electrode into the SWNT valence band,<sup>10</sup> the measured current is small and the device is said to be in the “OFF-state”. More negative gate voltages will decrease the SB width and increase hole transport into the SWNT, the device is said to turn on and the current will increase; towards very negative gate voltages, the current will saturate and the device is said to be in the “ON-state”. Sweeping the gate voltage at a constant  $V_{SD}$  creates a current (or conductance) *versus* gate voltage curve,  $I-V_G$  (or  $G-V_G$ ) called a transistor transfer characteristic. NTFET devices consisting of a network of SWNTs between the source and drain electrodes, as shown in Fig. 1C, will invariably contain metallic nanotubes and demonstrate non-zero current (conductance) at very positive gate voltages. Fig. 1D is a  $G-V_G$  transfer characteristic obtained with a NTFET device composed of a random network of SWNTs between interdigitated Ti/Au S–D electrodes and a Si back gate electrode; here  $V_{SD} = 0.05$  V.

The non-zero conductance at positive extremes of the  $V_G$  sweep is a result of the metallic SWNTs present in the

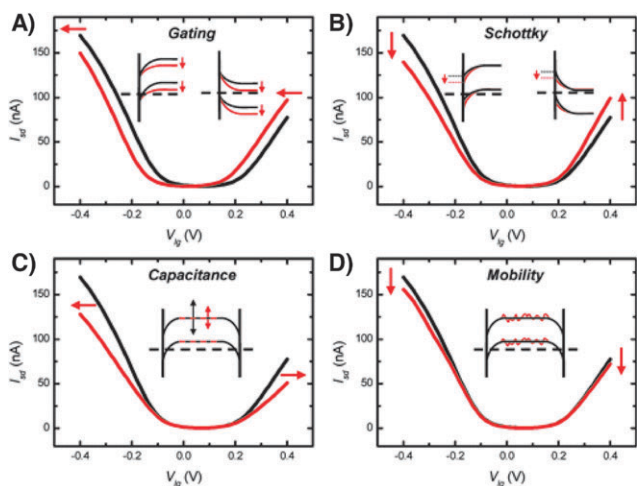


**Fig. 2** The calculated changes in a NTFET transfer characteristic before (black curve) and after (red curve) protein adsorption; the insets show the resulting effect on the SWNT band structure. (A) Electrostatic gating of the SWNT results in a shift in the transfer characteristic without a change in the transconductance. (B) Schottky barrier modification results in opposing effects for hole and electron transport, subsequently an increase in n-type conductance (positive gate voltages) and a decrease in p-type conductance (negative gate voltages) occurs. Changes in (C) capacitance and (D) mobility have similar effects on the NTFET transfer characteristic; however at high coverage (here 90%) changes in the capacitance have a more pronounced effect. (Reproduced with permission from ref. 12, copyright 2008 American Chemical Society.)

conduction channel. An alternative device design allows NTFET operation in liquid environments where the electrochemical potential of the liquid is controlled with a gate electrode;<sup>11</sup> similar to a back gated NTFET, the current (conductance) is modulated by sweeping the gate voltage (liquid potential) between positive and negative voltages. The liquid gated NTFET device design is illustrated in Fig. 1E and is useful for monitoring real-time interactions between SWNTs and biological molecules in a liquid environment.

### Mechanisms of NTFET sensor response

An advantage of using NTFET devices over more simple chemiresistors (where the SWNT is simply used to bridge two metal electrodes) is that NTFETs can differentiate between mechanisms prompting device response. The exact mechanistic origins of NTFET device response remains a heatedly debated topic in the literature. For example, Dekker and co-workers<sup>12</sup> recently published a report that identified four distinct phenomena responsible for NTFET-based sensor response. Mathematically, the NTFET conductance,  $\sigma$ , is defined as the number and mobility of charge carriers in the SWNT, denoted as  $n$  and  $\mu$ , respectively, such that  $\sigma = ne\mu$  where  $e$  is the elemental charge.<sup>2</sup> For example, a change in  $n$  (charge transfer) will result in a shift in the  $G-V_G$  (or  $I-V_G$ ) transfer characteristic and change in the device conductance (or current) at any arbitrary gate voltage (Fig. 2A). More specifically, donation of electronic density into the p-type SWNT will result in a shift of the transfer characteristic

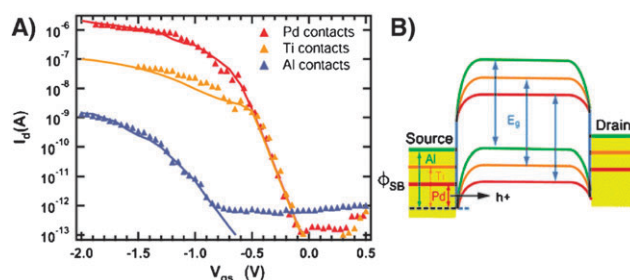


**Fig. 3** (A) NTFET devices with metal electrodes of lower work function experienced either a decrease in the maximum current and/or a shift in the NTFET transfer characteristic towards more negative voltages. (B) A band diagram explaining the experimental findings shown in part A where a smaller work function results in a larger SB for hole ( $h^+$ ) transport into the SWNT valence band. (Reproduced with permission from ref. 14, copyright 2005 American Chemical Society.)

towards more negative gate voltages and result in decreased current at any arbitrary gate voltage. Alternatively, Fig. 2B illustrates the effect of Schottky barrier modification on NTFET behavior where molecular adsorption on the electrode changes the local work function of the metal and alters the band alignment of the SWNT. Because different barriers exist for hole and electron transport they suggest Schottky barrier modification will create an asymmetric change for n- and p-type conduction.

A change in the device capacitance is shown in Fig. 2C. This example is modeled on the behavior of a liquid gated NTFET where molecular adsorption lowers the local permittivity relative to the electrolyte solution, and thereby reduces the efficiency of the liquid gate. Interestingly, they claim that a near complete coverage on the SWNT surface is needed to fully observe this effect. Lastly, a change in charge mobility,  $\mu$ , will result in a reduction in the slope of the transfer characteristic, called the transconductance; this leads to a decrease in the device conductance without shifting the  $G-V_G$  to lower gate voltages, as shown in Fig. 2D.

Currently, most reports of NTFET-based sensors cite charge transfer or Schottky barrier modification as the dominant mechanism responsible for device response. To further illustrate the influence of Schottky barrier modification on the behavior of NTFET devices, recall that NTFET devices behave as Schottky barrier transistors;<sup>13</sup> this means that the electronic behavior of the device is intimately related to the work function of the electrode. Avouris and co-workers reported that NTFET transfer characteristics can experience shifts based on a change in the work function of the device electrodes.<sup>14</sup> They found that NTFET devices constructed with lower metal work function electrodes exhibited lower ON-state current and/or a shift in the transfer characteristic towards more negative gate voltages, as shown in Fig. 3A. The authors used the band structure diagram of the SWNT-metal contact shown in Fig. 3B to provide an explanation for their experimental results. A larger SB will require more negative gate voltages to transport a hole ( $h^+$ ) into the SWNT valence band, resulting in a device with lower maximum ON-state current. This has very serious implications towards monitoring molecular systems with NTFET devices because a supposedly

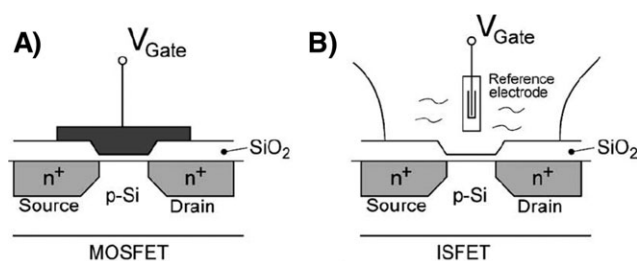


**Fig. 4** Schematic diagram of: (A) a metal oxide semiconductor FET (MOSFET) and (B) an ion selective FET (ISFET). (Reproduced with permission from ref. 17, copyright 2003 Elsevier Ltd.)

electron donating molecule may create a negative shift in the transfer characteristic by simply lowering the work function of the device electrode. In NTFET response, the distinction between electronic interaction with the SWNT and SB modification is subtle; however Dekker and co-workers recent report<sup>12</sup> can serve as a guide for researchers determining the mechanistic origins of sensor response. Using relevant examples from the CNT literature, we show a thread of commonality in NTFET sensor reports in that most cases the device response can be explained in terms of the four basic mechanistic descriptions.

### Advantage of NTFETs over other semiconductor technologies

NTFETs differ from the traditional metal oxide semiconductor FETs (MOSFET) in that device conductance is modulated through the SB at the SWNT–metal interface.<sup>10</sup> In a MOSFET, the conductance of the device is controlled by applying a  $V_G$  to the surface of the SiO<sub>2</sub> insulation layer separating the gate and Si conduction channel. Once a sufficiently positive  $V_G$  is applied a region of mobile charges in the underlying Si layer forms between the S–D electrodes; this is called an inversion layer, and by turning the initially p-type Si into an n-type conductor the device will turn on and current will flow.<sup>15</sup> A schematic of a typical top-gated MOSFET device is illustrated in Fig. 4A.

Two examples of Si-based MOSFET sensors are the gas sensitive MOSFET and the ion sensitive FET (ISFET).<sup>15</sup> The traditional example of a gas-sensitive MOSFET is the H<sub>2</sub> sensitive FET constructed with a Pd gate first reported by Lundström and co-workers in 1974.<sup>16</sup> Device response relied on gas interaction with the device gate electrode, which was located on top of the semiconducting SiO<sub>2</sub> conduction channel. For example, H<sub>2</sub> dissociatively adsorbs, and dissolves into the Pd surface at room temperature. The dissolved H atoms would then diffuse to the Pd–SiO<sub>2</sub> interface, resulting in a change in the Pd work function and a shift in the transistor transfer characteristic. The change in work function was dependent on the concentration of the H<sub>2</sub> gas, creating a usable sensor response. The ISFET was developed in the early 1970s for use in liquid environments and is illustrated in Fig. 4B. Operation of an ISFET is similar to a typical MOSFET except the device conductance is controlled through the electrochemical potential of a liquid environment using a reference electrode instead of an insulated gate electrode. In

this configuration the ISFET performance is then controlled by the chemical environment, and shows sensitivity to pH and metal ions in solution.

The past 30 years has seen vibrant development of chemically sensitive FETs (CHEMFETs),<sup>17,18</sup> which incorporate a chemically selective layer or membrane into the MOSFET or ISFET device architecture. While these devices have been described as the “potentiometric sensor of the future” they have found little commercial success.<sup>18</sup> NTFET devices, on the other hand, show several intrinsic properties that make them an attractive alternative to more traditional semiconductor FET architectures. For example, NTFETs constructed in a top-gate configuration, similar to the MOSFET shown in Fig. 4A, show appreciably larger ON-state current ( $I_{ON}$ ) and transconductance, as well as a smaller OFF-state current ( $I_{OFF}$ ) as compared to a state of the art high-performance p-channel Si MOSFET.<sup>19</sup> Table 1 provides a quantitative comparison between several of the NTFET and Si-MOSFET properties, where  $I_{ON}$ ,  $I_{OFF}$  and the transconductance are given per unit length ( $\mu\text{m}$ ). Even though the authors admit the device performance has not yet been optimized, the NTFET demonstrates a nearly four-fold increase in the  $I_{ON}$ , more than a two-fold increase in the transconductance, and an  $I_{OFF}$  approximately half that of the Si-MOSFET device; clearly the NTFET has great potential for success in applications previously dominated by Si-technologies. Towards sensor applications, increased ON and OFF state currents combined with a larger transconductance will result in a larger response for any given shift in the transfer characteristic. This larger signal transduction means the NTFET will behave as a much more sensitive sensor device.

In addition to enhanced electrical transport properties, there are several structural characteristics of CNTs, and particularly SWNTs, that set them apart as an excellent choice for sensor applications. For example, the large percentage of surface atoms makes the SWNT extremely sensitive to its local chemical environment. Additionally, the SWNT diameter is comparable to large biological molecules, enabling it to directly “wire into” the system of interest, as shown in Fig. 5A and B.<sup>20,21</sup> Lastly, the aromatic all-carbon structure of the SWNT allows for a vast array of possible chemical functionalization schemes.<sup>22</sup> This presents the opportunity for molecule specific detection through controlled chemical reactions occurring at the SWNT surface, as well as label-free biological detection through specific binding events. These unique characteristics allow NTFET devices to perform as an extremely sensitive platform technology to study diverse chemical and biological systems through the use of selective chemistry at the surface of the SWNT conduction channel.

### Current protein and DNA analysis technology

Current methods for protein and DNA analysis include optical spectroscopy, mass spectrometry, and gel electrophoresis.<sup>23–26</sup> While these methods have exquisite sensitivity, their throughput is somewhat slow and the instrumentation can be quite costly. Furthermore, these methods need well-trained operators, they typically require additional sample preparation, and because of their slow throughput realtime,

**Table 1** Electronic characteristics of a p-type NTFET and a Si-MOSFET<sup>a</sup>

	p-Type NTFET	p-Channel Si MOSFET
Gate length/nm	260	15
Gate oxide thickness/nm	15	1.4
$V_t/V$	-0.5	$\sim -0.1$
$I_{ON}/\mu A \mu m^{-1}$	2100	265
$I_{OFF}/nA \mu m^{-1}$	-150	$< -150$
Transconductance/ $\mu A \mu m^{-1}$	2321	975

<sup>a</sup> Data from ref. 19.

continuous sample analysis becomes a problem. Gel electrophoresis may seem a more attractive technique because of its lower cost, however it is more labor intensive which introduces the possibility for inadvertent sample contamination.

In recent years, there has been an emphasis on the design of so-called “lab on a chip” devices capable of rapid analysis of samples containing biological materials.<sup>27,28</sup> The benefits of such an analytical platform is the possibility of in-field analysis of biological samples without the need for further sample preparation—greatly reducing the risk of inadvertent contamination. One approach towards this end is the use of miniaturized biosensors that utilize specific recognition events to transduce an electronic response.<sup>23,27,28</sup> While this method is highly sensitive, it still requires sample amplification for detection of target species.

Ideally, one would want an analytical platform that was easy to operate, relatively inexpensive, and did not require further sample preparation. In this tutorial review, we describe

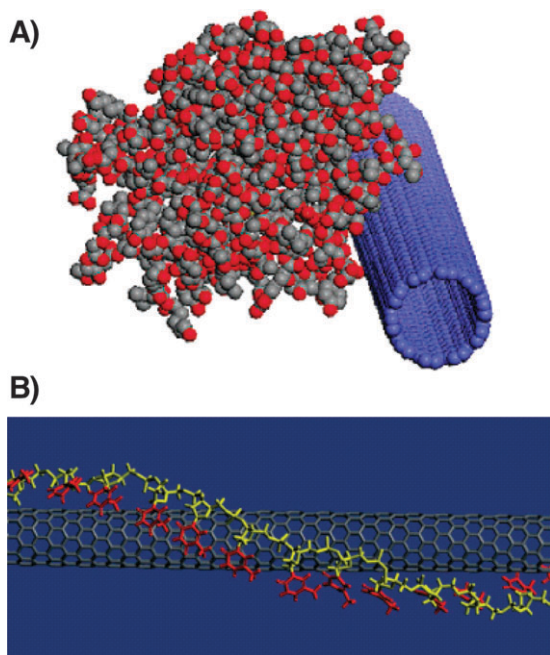


**Fig. 5** (A) Cartoon comparing the sizes of a SWNT and a streptavidin molecule, where nitrogen atoms are colored red. (Reproduced with permission from ref. 20, copyright 2004 American Chemical Society.) (B) A SWNT wrapped with DNA. (Reproduced with permission from ref. 21, copyright 2003 Macmillan Publishers Ltd.)

how CNTs have the potential to fill this role through the use of NTFET-based biosensors for DNA and protein analysis.<sup>4,29,30</sup>

## Detection of biological species using NTFETs

The detection of biological molecules using CNTs is a rapidly growing field. While electrochemical-based CNT biosensors have been reported, we will restrict this discussion specifically to NTFET-based protein and DNA detection and analysis.<sup>4,31–34</sup> However, the interested reader is directed towards several excellent reviews concerning the use of CNT electrochemistry for sensor applications.<sup>30,35,36</sup> The goal of NTFET biological sensors is ultimately the design of rugged, low cost and user-friendly analytical platforms for in-field analysis of biological samples.

### Protein detection with NTFETs

The past several years have seen many impressive reports of protein detection using SWNT NTFET sensors, including the development of specific biosensors,<sup>37</sup> the electronic detection of viral proteins,<sup>38</sup> and kinetic studies of protein antibody binding using top-gated NTFET devices with low nM detection limits.<sup>39</sup>

Dai and co-workers reported that SWNTs non-covalently functionalized with linker molecules could effectively immobilize protein molecules.<sup>40</sup> Later, they used this approach to demonstrate a protein specific sensor platform.<sup>41</sup> We have also shown that NTFET devices can be used to monitor biomolecular recognition events such as specific biotin–streptavidin binding, as represented in Fig. 6A.<sup>42</sup> NTFETs were non-covalently functionalized with a layer of poly(ethylene imine) (PEI) and poly(ethylene glycol) (PEG) to prevent non-specific binding between the SWNT and streptavidin protein molecules. The addition of the PEI–PEG layer turned the NTFET into an n-type transistor, presumably from the donation of electronic density into the SWNT valence band. Subsequent biotinylation of the polymer layer returned the NTFET back to a p-type device through chemical modification of the amine groups in the polymer; the biotin served as binding sites for streptavidin protein molecules. To monitor the binding events, polymer–biotin functionalized NTFET devices were submerged in a 2.5  $\mu M$  solution of 10 nm Au nanoparticle labeled streptavidin in a 0.01 M phosphate buffered saline solution of pH 7.2 at room temperature for 15 minutes. The AFM image in Fig. 6B shows the Au nanoparticle labeled streptavidin immobilized on the SWNT surface and underlying SiO<sub>2</sub> substrate.

Electronically, the interaction between an unfunctionalized NTFET and streptavidin results in a decrease in the device ON-state current and a shift in the  $I-V_G$  curve towards more negative gate voltages, as shown in Fig. 6C. The response of the polymer–biotin functionalized NTFET to streptavidin was different, and the streptavidin binding resulted in a significant decrease in the slope of the  $I-V_G$  curve, as illustrated in Fig. 6D. The difference between the bare and polymer–biotin functionalized NTFET response to streptavidin binding is significant and suggests two unique mechanisms govern the device response. For example, the negative shift in the  $I-V_G$  transfer characteristic and decreased ON-state current of the

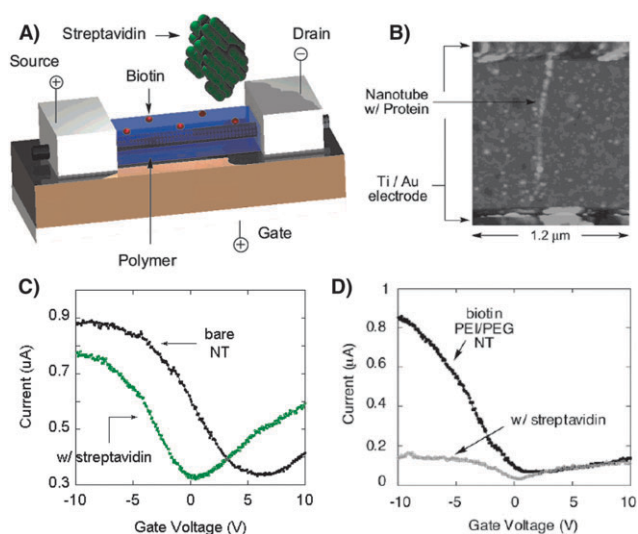


**Fig. 6** (A) A cartoon of a polymer–biotin functionalized NTFET device undergoing a biorecognition event between the biotinylated polymer and a streptavidin protein molecule (dimensions are not to scale). (B) AFM image of the polymer–biotin coated NTFET device after exposure to Au nanoparticle labeled streptavidin molecules.  $I$ – $V_G$  transfer characteristics of (C) an unfunctionalized and (D) polymer–biotin functionalized NTFET before and after the addition of streptavidin. (Reproduced with permission from ref. 42, copyright 2003 American Chemical Society.)

bare NTFET device suggests streptavidin adsorption resulted in a donation of electronic density into the SWNT. On the other hand, the decreased slope in the  $I$ – $V_G$  transfer characteristic of the biotin–polymer functionalized NTFET suggests streptavidin binding resulted in a reduction in charge mobility. We suggested that the biotin–streptavidin binding event created geometric deformations in the polymer structure, this would introduce charge scattering sites along the SWNT and reduce the ON-state current without shifting the  $I$ – $V_G$  transfer characteristic. The observed NTFET behavior very closely resembles that depicted in Fig. 2A and D.<sup>12</sup>

The potential for this type of sensor architecture is the possible detection of a single binding event, *i.e.* single molecule detection. Using the current experimental setup the signal to noise ratio of these devices was approximately 10, and based on the AFM image presented in Fig. 6B we concluded that approximately 100 streptavidin molecules were bound to an individual SWNT. Based on these numbers a theoretical detection limit of only 10 streptavidin molecules was achieved, and further development of this technology could obtain the goal of single molecule detection.

Using NTFET devices, Bradley *et al.* conducted quantitative experiments to calculate the charge transfer from streptavidin adsorbed on the SWNT surface.<sup>20</sup> By studying protein adsorption with back gated NTFET devices in dry environments and liquid gated NTFET devices, they concluded that changes in the NTFET transfer characteristic stemmed from charge transfer with the SWNT conduction channel. Protein adsorption resulted in negative shifts in the device transfer characteristic which we previously attributed to electronic donation into the SWNT.<sup>42</sup> Using  $\text{NH}_3$  as a model, it was

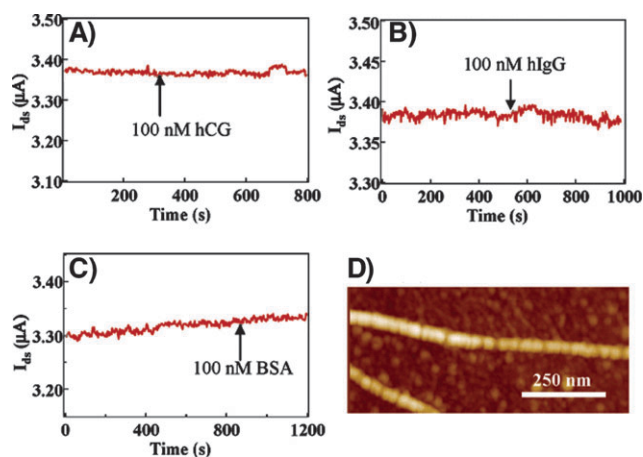


**Fig. 7** NTFET devices consisting of electrodes passivated with thiolated poly(ethylene glycol) did not show response to 100 nM (A) hCG, (B) hIgG or (C) BSA even though subsequent AFM imaging (part D) revealed the SWNT conduction channels were coated with adsorbed protein. (Reproduced with permission from ref. 43, copyright 2004 American Chemical Society.)

assumed that each of the approximately 4000 amine groups per streptavidin molecule in contact with the SWNT donated 0.04 electrons into the SWNT valence band. From this estimated value, a calculated shift of  $-50$  mV was expected in liquid gated NTFET devices after incubation with streptavidin. Experimentally a value of  $-60 \pm 3$  mV was observed in liquid gated NTFET devices, suggesting  $\text{NH}_3$  is an appropriate model for understanding the interaction between SWNTs and larger molecules with many amine groups.

Growing interest has surrounded the potential of SWNT devices to electronically monitor protein binding events; however Dai and co-workers investigated whether the SWNT is transducing changes in its local charge environment, or if protein activity actually serves to modify device Schottky barriers.<sup>43</sup> For example, by covalently attaching thiol terminated PEG to the device electrodes they were able to prevent protein interaction with the metal (Fig. 7A–D). The authors contend this type of electrode passivation is advantageous because it produces an even monolayer that extends to the edges of the electrode while leaving the SWNTs pristine. Furthermore, passivation schemes are more reliable when investigating biological systems because the molecules of interest are much larger than gas molecules, and are much less likely to diffuse through small pinholes in the passivation layer.

Dai and co-workers found that unpassivated NTFET devices showed significant response to several proteins including human chorionic gonadotropin (hCG), polyclonal human IgG (hIgG) and bovine serum albumin (BSA); however devices with passivated electrodes did not show response to protein exposure, as shown in Fig. 7A–C. While protein exposure did not result in electronic response in electrode passivated devices, subsequent AFM imaging revealed obvious protein adsorption along the SWNT length (Fig. 7D). The authors contend the lack of electronic response is a result of the polymer passivation layer preventing protein adsorption on the electrode surface, subsequently inhibiting

the modification of the device Schottky barrier. This is an excellent example of how identification and exploitation of one of the four basic NTFET response mechanisms can lead to selective sensor performance.

An interesting experiment was reported by Byon and Choi<sup>44</sup> who measured the response of NTFET devices with extended Schottky contact areas to proteins such as SpA (derived from *Staphylococcus aureus*), streptavidin, mouse antibody  $\beta$ -hCG, human chorionic gonadotropin (hCG), and rabbit immunoglobulin G (IgG). Extended area Schottky contacts were fabricated by evaporating Cr/Au layers at a 23° angle through a shadow mask onto a Si/SiO<sub>2</sub> substrate. The resulting NTFET devices showed very little conductance modulation with the applied gate voltage; however they did show strong response ( $\geq 1\%$ ) to pM concentrations of proteins. The authors suggest the high sensitivity is due to the increased electrode area for protein adsorption, and subsequent work function modification. This report is a clever example of how identification and exploitation of the dominant response mechanism can be used to maximize the device sensitivity.

Recently Minot *et al.* reported what they claim to be unambiguous determination of charge transfer from BSA proteins into the valence band of SWNTs.<sup>45</sup> In this report they investigated the influence of the physical structure of the gate electrode on the behavior of liquid gated NTFET devices during protein adsorption. They contend the use of a Pt reference electrode as the liquid gate electrode can lead to

distortion of the true device transfer characteristic because the potential barrier between the Pt wire and the solution is sensitive to molecular interaction. To alleviate this problem a conventional Ag/AgCl reference electrode was used to control the electrochemical potential placed on the SWNT. An Ag/AgCl reference electrode is constructed with a small piece of fritted glass, which they suggest creates a barrier towards BSA entering the electrode and reaching the metal surface. With this experimental setup, they found BSA adsorption induced a shift in the liquid gated NTFET transfer characteristic of  $-15$  mV, which they directly attribute to charge transfer between the SWNT and protein. This report may add a new level of complexity to liquid phase NTFET operation because it suggests device response can be influenced by molecular interactions with the device S–D and/or gate electrodes, but it also provides another tool for researchers to more finely tune their device performance and more accurately assess the mechanistic origins of sensor response.

#### DNA detection with NTFETs

In recent years, the interaction between SWNTs and DNA molecules has obtained much attention. Computational,<sup>46</sup> as well as spectroscopic and kinetic studies,<sup>47</sup> agree that DNA adsorption on SWNT occurs and that changes in conformation should be transduced through the SWNT electronic structure.

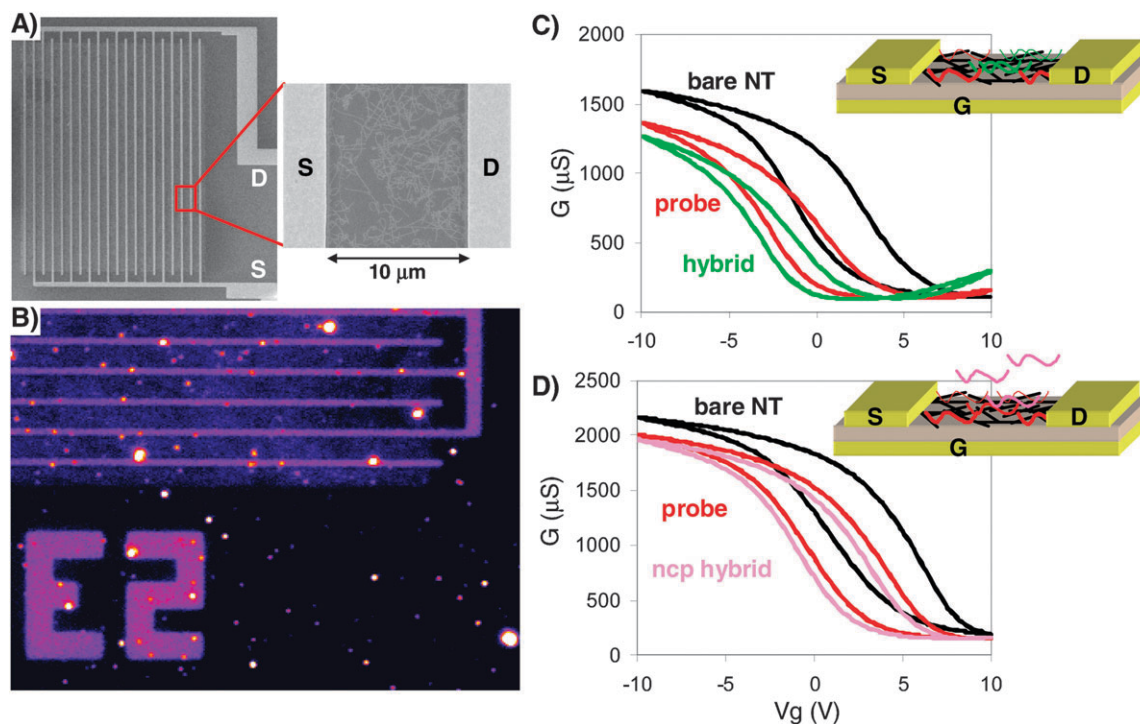


**Fig. 8** (A) SEM images of an interdigitated NTFET device composed of a random network of SWNTs as a conduction channel between S–D electrodes; the separation between S–D electrodes is 10 μm. (B) Fluorescent microscope image of an interdigitated NTFET device with the unlabeled DNA capture probes after incubation with FITC-labeled complementary DNA target (5′-FITC-ATT GTT ATT AGG-3′); the separation between S–D electrodes in this device is 10 μm. NTFET transfer characteristics and schematic drawings of DNA-functionalized NTFET devices (C) before (bare SWNT) and after incubation with 12-mer oligonucleotide capture probes (5′-CCT AAT AAC AAT-3′), as well as after incubation with the complementary FITC-labeled DNA target, and (D) before and after incubation with dA<sub>12</sub> captures as well as after incubation with a non-complementary DNA target.  $G$ – $V_G$  measurements were taken at a constant S–D bias of 50 mV. (Reproduced with permission from ref. 48, copyright 2006 National Academy of Sciences of the United States of America.)

We recently reported that DNA hybridization can be monitored in a label-free manner using the electronic response of NTFET devices.<sup>48</sup> Interdigitated NTFETs (Fig. 8A) were incubated in an unlabeled 12-mer oligonucleotide capture probe solution. To visually confirm hybridization, the capture probe was incubated with an FITC-labeled complementary DNA target. After incubation with the fluorescently labeled complementary strand, a signal could be seen in the SWNT network between the interdigitated device electrodes, as shown in Fig. 8B. This clearly shows that DNA hybridization occurred between the SWNT immobilized capture probes and the fluorescently labeled target strands.

Electronically, the hybridization event could be monitored based on changes in the NTFET transfer characteristic, shown in Fig. 8C. The  $G-V_G$  transfer characteristic of bare NTFETs experienced a shift towards more negative gate voltages and a decrease in conductance after functionalization with the oligonucleotide capture probe. We attributed the changes in the NTFET transfer characteristic to electronic donation *via* non-covalent  $\pi$ - $\pi$  attachment of the DNA strand, which is very similar to the behavior observed during the interaction of SWNTs and streptavidin.<sup>20</sup> Once a complementary strand was introduced, a further shift in the  $G-V_G$  curve and decrease in conductance was observed, which we rationalized was a result of DNA hybridization. Somewhat intuitively, this behavior was not observed with NTFET devices exposed to non-complementary DNA strands, as shown in Fig. 8D, and indicates DNA hybridization on the SWNT network was responsible for the observed changes in the NTFET transfer characteristics. Moreover, we found that the addition of metal salt cations, specifically  $\text{Na}^+$  and  $\text{Mg}^{2+}$ , facilitates the DNA hybridization events. Complementary spectroscopic evidence for the detection of DNA conformational changes on SWNTs was reported by Strano and co-workers,<sup>49</sup> who found changes in SWNT immobilized DNA in the presence of  $\text{Ca}^{2+}$ ,  $\text{Co}^{2+}$ ,  $\text{Hg}^{2+}$  and  $\text{Mg}^{2+}$  cations produced shifts in the SWNT fluorescence spectra. The results of this experiment are very significant because they give support to our claim that the SWNT conduction channel of the NTFET device is sensitive to changes in the local charge environment upon changes in the conformation (hybridization) of the immobilized DNA strand.

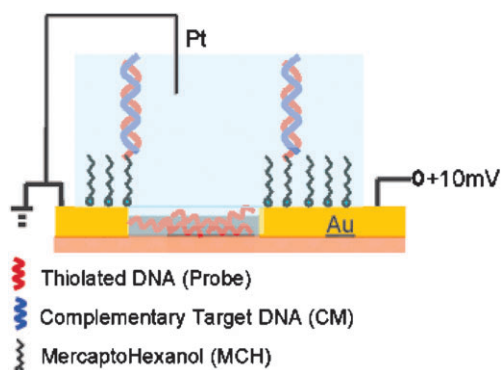


**Fig. 9** Experimental setup used by Tang *et al.* to investigate the hybridization of thiolated DNA strands using a liquid gated NTFET device. (Reproduced with permission from ref. 50, copyright 2006 American Chemical Society.)

Tang *et al.* reported that NTFET response to DNA hybridization is a direct result of modification of the work function of the Au device electrodes.<sup>50</sup> NTFET devices with Au electrodes covered with a self-assembled monolayer (SAM) of mercaptohexanol (MCH) were used to study the hybridization of complementary strands of thiolated DNA; their experimental design is shown in Fig. 9, where a Pt wire acted as a liquid gate electrode. Using quartz crystal microbalance (QCM) and X-ray photoelectron spectroscopy (XPS) measurements they found that DNA hybridization did not occur on the SWNTs, but rather it occurred only on the MCH covered electrodes. To induce DNA hybridization on the SWNT, they functionalized the SWNT surface with a phospholipid-PEG maleimide linker molecule, which was used to immobilize the thiolated DNA capture probe. QCM and XPS measurements confirmed hybridization of the DNA strands attached to the linker layer, but the hybridization produced no electronic response. Based on these results, Tang *et al.* concluded that DNA hybridization induced a change in the metal work function of the device electrodes, and device response did not originate from a change in the electronic density of the SWNT valence band.

Gui *et al.* have recently reported that NTFET response to DNA hybridization can be attributed to a combination of charge transfer with the SWNT and SB modification;<sup>51</sup> however they claim SB modification is the dominant mechanism driving the device response. Their experiments were conducted with NTFET devices composed of interdigitated Au or Cr electrodes with a network of SWNTs acting as the conduction channel. Using fluorescently labeled target strands they found that DNA hybridization occurred on the SWNT network between the NTFET interdigitated electrodes. Furthermore, they attributed a weak fluorescent signal from the device electrodes to non-radiative energy transfer from the fluorescent label to the metal electrode. Similar to our report they found that immobilization of a capture probe DNA strand shifted the NTFET transfer characteristic towards more negative gate voltages and a decrease in the maximum device current. At a fixed gate voltage of  $-10$  V, the Au contacted devices experienced a  $\sim 55\%$  decrease in current while the Cr contacted devices experienced a nearly 100% decrease in current. After DNA hybridization, Au contacted devices experienced a further decrease in device current while Cr contacted devices actually experienced an increase in device current. This result suggests that charge transfer with the SWNT may not be the only mechanism governing NTFET response, and that the device electrode may play a significant role in the observed electrical response.

Additionally, Gui *et al.* conducted area-selective passivation experiments to understand how DNA interaction with the device electrode affected the observed electrical response. For example, Fig. 10A shows the transfer characteristics of a NTFET device with a single Au electrode and a portion of the SWNT network exposed; the remainder of the device was passivated with photoresist, as shown in the inset. They found that DNA immobilization shifted the  $I-V_G$  curve towards more negative gate voltages and created a decrease in the device current. The addition of a complementary DNA strand, and subsequent hybridization resulted in a further shift in the  $I-V_G$  curve towards more negative gate voltages and decreased device conductance.



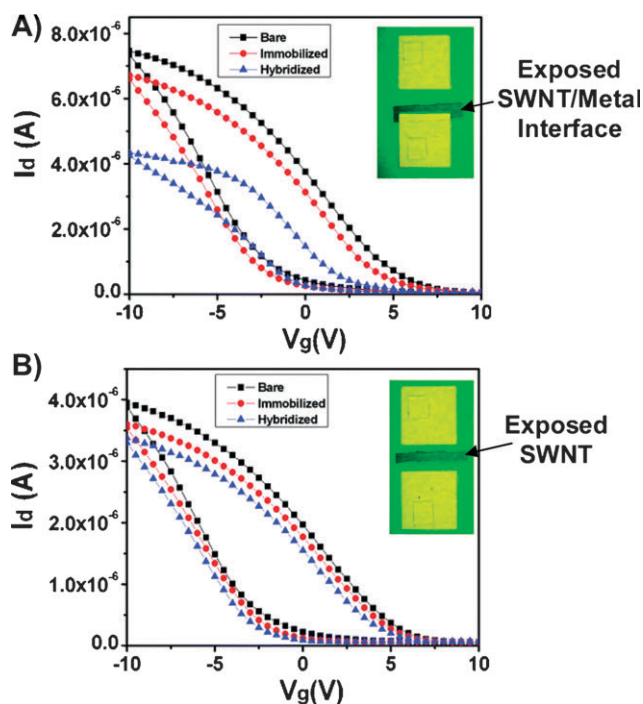


**Fig. 10** Transfer characteristics of photos resist passivated NTFET devices before (black curve), and after DNA immobilization (red curve) and hybridization (blue curve). (A) A device with only one electrode and a small section of SWNT network exposed; as shown in the inset. This device responded to both DNA immobilization and hybridization. (B) A device with both electrodes passivated and only a small section of SWNT network exposed in the center of the device; as shown in the inset. This device did not demonstrate significant response to either DNA immobilization or hybridization. (Reproduced with permission from ref. 51, copyright 2007 American Chemical Society.)

Furthermore, it appears that DNA hybridization also decreased the slope of the  $I-V_G$  curve, indicating a reduction in the charge mobility through the addition of charge scattering sites on the SWNT surface. An identical experiment was conducted using a passivated NTFET device that had only a small segment of the SWNT network exposed in the center of the device; the device electrodes and a majority of the SWNT network were covered with photoresist (inset of Fig. 10B). This device did not demonstrate significant response to either DNA immobilization or hybridization, as shown with the transfer characteristic in Fig. 10B. From this set of experiments the authors concluded that charge transfer with the SWNT network does not play a significant role in the detection of DNA immobilization or hybridization. They contend that the dominant mechanism behind the device response is modification of the metal electrode work function; however they do concede that charge transfer with the portion of the SWNT network immediately adjacent to the electrode (within the depletion region) may play a role in the electronic response.

## Conclusions

The outlook for NTFET devices is bright because the inherent environmental sensitivity of the CNT conduction channel makes them excellent candidates for the development of

compact and inexpensive field-usable analytical platforms for label-free detection and analysis of biological species such as proteins and DNA. Moreover, NTFET devices have shown promise in label-free detection of biological molecules which could aid the development of proteomic and genomic diagnostic tools.

As outlined, many researchers have devoted a considerable amount of attention to the fundamental mechanisms underlying NTFET response to biological species. The intense interest thus far demonstrated in NTFET sensor platforms will only further develop this field and ultimately heighten chemical sensitivities. The distinction between the mechanistic origins of NTFET response are subtle, and quantitatively distinguishing between them can be a daunting task. However, a fundamental understanding of device response is very important because it will allow researchers to develop better sensors.

The NTFET has shown great promise in becoming a platform technology for studying a vast array of biological systems. The nano-scale dimensions of the CNT conduction channel allow the design and fabrication of novel electronic architectures that are inherently sensitive to their local molecular environment. Chemical functionalization further exploits the NTFET sensitivity by adding a new dimension of analyte selectivity. The past ten years have seen an amazing progress in NTFET capability, and one can only speculate on what exciting new developments will emerge in the future.

## References

- 1 S. J. Tans, A. R. M. Verschueren and C. Dekker, *Nature*, 1998, **393**, 49.
- 2 R. Martel, T. Schmidt, H. R. Shea, T. Hertel and P. Avouris, *Appl. Phys. Lett.*, 1998, **73**, 2447.
- 3 N. Sinha, J. Ma and J. T. W. Yeow, *J. Nanosci. Nanotechnol.*, 2006, **6**, 573.
- 4 B. L. Allen, P. D. Kichambare and A. Star, *Adv. Mater.*, 2007, **19**, 1439.
- 5 T. W. Odom, J.-L. Huang, P. Kim and C. M. Lieber, *J. Phys. Chem. B*, 2000, **104**, 2794.
- 6 P. G. Collins, K. Bradley, M. Ishigami and A. Zettl, *Science*, 2000, **287**, 1801.
- 7 V. Derycke, R. Martel, J. Appenzeller and P. Avouris, *Appl. Phys. Lett.*, 2002, **80**, 2773.
- 8 A. Zangwill, *Physics at Surfaces*, Cambridge University Press, Cambridge, UK, 1988.
- 9 E. S. Snow, J. P. Novak, P. M. Campbell and D. Park, *Appl. Phys. Lett.*, 2003, **82**, 2145.
- 10 J. Appenzeller, J. Knoch, V. Derycke, R. Martel, S. Wind and P. Avouris, *Phys. Rev. Lett.*, 2002, **89**, 126801.
- 11 S. Rosenblatt, Y. Yaish, J. Park, J. Gore, V. Sazonova and P. L. McEuen, *Nano Lett.*, 2002, **2**, 869.
- 12 I. Heller, A. M. Janssens, J. Männik, E. D. Minot, S. G. Lemay and C. Dekker, *Nano Lett.*, 2008, **8**, 591.
- 13 S. Heinze, J. Tersoff, R. Martel, V. Derycke, J. Appenzeller and P. Avouris, *Phys. Rev. Lett.*, 2002, **89**, 106801.
- 14 Z. Chen, J. Appenzeller, J. Knoch, Y.-M. Lin and P. Avouris, *Nano Lett.*, 2005, **5**, 1497.
- 15 M. J. Madou and S. R. Morrison, *Chemical Sensing with Solid State Devices*, Academic Press, Inc., New York, USA, 1989.
- 16 I. Lundström, S. Shivaraman, C. Svenson and L. Lundkvist, *Appl. Phys. Lett.*, 1974, **26**, 55.
- 17 P. Bergveld, *Sens. Actuators, B*, 2003, **88**, 1.
- 18 J. Janata, *Electroanalysis*, 2004, **16**, 1831.
- 19 P. Avouris, J. Appenzeller, R. Martel and S. J. Wind, *Proc. IEEE*, 2003, **91**, 1772.

- 20 K. Bradley, M. Briman, A. Star and G. Grüner, *Nano Lett.*, 2004, **4**, 253.
- 21 M. Zheng, A. Jagota, E. D. Semke, B. A. Diner, R. S. Mclean, S. R. Lustig, R. E. Richardson and N. G. Tassi, *Nat. Mater.*, 2003, **2**, 338.
- 22 N. Niyogi, M. A. Hamon, H. Hu, B. Zhao, P. Bhowmik, R. Sen, M. E. Itkis and R. C. Haddon, *Acc. Chem. Res.*, 2002, **35**, 1105.
- 23 B. Leca-Bouvier and L. J. Blum, *Anal. Lett.*, 2005, **38**, 1491.
- 24 B. Doman and R. Aebbersold, *Science*, 2006, **312**, 212.
- 25 J. Tost and I. G. Gut, *J. Mass Spectrom.*, 2006, **41**, 981.
- 26 C. A. Hutchinson III, *Nucleic Acids Res.*, 2007, **35**, 6227.
- 27 M. A. Jobling and P. Gill, *Nat. Rev. Genet.*, 2004, **5**, 739.
- 28 K. M. Horsman, J. M. Bienvenue, K. R. Blasier and J. P. Landers, *J. Forensic Sci.*, 2007, **52**, 784.
- 29 W. Yang, P. Thordarson, J. J. Gooding, S. P. Ringer and F. Braet, *Nanotechnology*, 2007, **18**, 412001.
- 30 S. N. Kim, J. F. Rusling and F. Papadimitrakopoulos, *Adv. Mater.*, 2007, **19**, 3214.
- 31 K. Balasubramanian and M. Burghard, *Anal. Bioanal. Chem.*, 2006, **385**, 452.
- 32 E. Katz and I. Willner, *ChemPhysChem*, 2004, **5**, 1084.
- 33 G. Grüner, *Anal. Bioanal. Chem.*, 2006, **384**, 322.
- 34 J. V. Veetil and K. Ye, *Biotechnol. Prog.*, 2007, **23**, 517.
- 35 J. Wang, *Electroanalysis*, 2005, **17**, 7.
- 36 G. G. Wildgoose, C. E. Banks, H. C. Leventis and R. G. Compton, *Microchim. Acta*, 2006, **152**, 187.
- 37 K. Maehashi, T. Katsura, K. Kerman, Y. Takamura, K. Matsumoto and E. Tamiya, *Anal. Chem.*, 2007, **79**, 782.
- 38 Y.-B. Zhang, M. Kanungo, A. J. Ho, P. Freimuth, D. van der Lelie, M. Chen, S. M. Khamis, S. S. Datta, A. T. C. Johnson, J. A. Misewich and S. S. Wong, *Nano Lett.*, 2007, **7**, 3086.
- 39 M. Abe, K. Murata, A. Kojima, Y. Ifuku, M. Shimizu, T. Ataka and K. Matsumoto, *J. Phys. Chem. C*, 2007, **111**, 8667.
- 40 R. J. Chen, Y. Zhang, D. Wang and H. Dai, *J. Am. Chem. Soc.*, 2001, **123**, 3838.
- 41 R. J. Chen, S. Bansaruntip, K. A. Drouvalakis, N. W. S. Kam, M. Shim, Y. Li, W. Kim, P. J. Utz and H. Dai, *Proc. Natl. Acad. Sci. U. S. A.*, 2003, **100**, 4984.
- 42 A. Star, J.-C. P. Gabriel, K. Bradley and G. Grüner, *Nano Lett.*, 2003, **3**, 459.
- 43 R. J. Chen, H. C. Choi, S. Bangsaruntip, E. Yenilmez, X. Tang, Q. Wang, Y.-L. Chang and H. Dai, *J. Am. Chem. Soc.*, 2004, **126**, 1563.
- 44 H. R. Byon and H. C. Choi, *J. Am. Chem. Soc.*, 2006, **128**, 2188.
- 45 E. D. Minot, A. M. Janssens, I. Heller, H. A. Heering, C. Dekker and S. G. Lemay, *Appl. Phys. Lett.*, 2007, **91**, 93507.
- 46 X. Zhao and J. K. Johnson, *J. Am. Chem. Soc.*, 2007, **129**, 10438.
- 47 E. S. Jeng, P. W. Barone, J. D. Nelson and M. S. Strano, *Small*, 2007, **3**, 1602.
- 48 A. Star, E. Tu, J. Niemann, J.-C. P. Gabriel, C. S. Joiner and C. Valcke, *Proc. Natl. Acad. Sci. U. S. A.*, 2006, **103**, 921.
- 49 D. A. Heller, E. S. Jeng, T.-K. Yeung, B. M. Martinez, A. E. Moll, J. B. Gastala and M. S. Strano, *Science*, 2006, **311**, 508.
- 50 X. Tang, S. Bansaruntip, N. Nakayama, E. Yenilmez, Y.-I. Chang and Q. Wang, *Nano Lett.*, 2006, **6**, 1632.
- 51 E. L. Gui, L. J. Li, K. Zhang, Y. Xu, X. Dong, X. Ho, P. S. Lee, J. Kasim, Z. X. Shen, J. A. Rogers and S. G. Mhaisalkar, *J. Am. Chem. Soc.*, 2007, **129**, 14427.